FATIGUE DAMAGE IN SPHEROIDAL GRAPHITE CAST IRON (SGI)

Y.Nadot* J.Mendez* N.Ranganathan* and A.S.Béranger**

Spheroidal Graphite cast Iron materials contain different types of heterogeneities in the microstructure which can explain important scatter in fatigue lives. Fatigue tests are conducted on as-cast cylindrical samples and the defect that initiate failure is carefully observed. Fatigue crack growth curves and linear elastic fracture mechanic concepts were used to calculate the fatigue life of a sample considering heterogeneities as cracks in a uniform stress field. Predictions are found to be in good agreement with experimental results for low cycle fatigue but not for high cycle fatigue. Results are discussed considering the defect parameters (size and geometry) and the stress level.

INTRODUCTION

SGI is a useful material for industrial applications : mechanical properties are similar to those of commonly used steels and castability is better than for low carbon steels. This is the reason why they are used in the automotive industry for engine and safety components (ex : crankshafts and suspension arms). However, due to casting process, microstructural heterogeneities are found both in industrial and laboratory castings. It is therefore necessary to characterize the fatigue damage mechanisms resulting from these defects. The purpose of this study is to investigate the application of Fatigue Crack Growth (FCG) results to natural short cracks in order to assess the fatigue life of SGI components. This paper reports the results of the long FCG behaviour of SGI and the characteristics of crack initiation and growth of small cracks observed developping on cylindrical samples. The results obtained are discussed considering the validity of the fracture mechanic approach.

* Laboratoire de Mécanique et de Physique des Matériaux - URA CNRS 863
ENSMA - Site du Futuroscope BP 109 - 86960 FUTUROSCOPE cedex FRANCE
** RENAULT SA Direction de la recherche
860 Quai de Stalingrad 92109 BOULOGNE BILLANCOURT cedex FRANCE

MATERIAL

SGI used in the present study has been provided by Renault SA. The matrix contains 95% ferrite and 5% pearlite, the volumic fraction of nodules is 10% with a ferrite grain size of 50 µm and a graphite size of 15 µm. Mechanical properties are : E=180 GPa, σ_y=380 MPa and UTS=510 MPa. The fatigue limit at R=0.1 in tension is 222 +/- 30 MPa. Fig.1 shows the microstructure of the as cast material. The bulk matrix has a homogeneous distribution of nodules in the ferrite matrix. SGI contains two kinds of heterogeneities. Near surface cast defects : dross defects produced by components that take part in the casting process (fig. 2). Internal defect : microshrinkages less than 500 µm.

CRACK GROWTH BEHAVIOUR

The material tested here was taken from the center of a casting block : the cast surface was 5 mm machined off in order to dispense with the surface heterogeneities so that the present results concern only the bulk matrix. Only a few microshrinkages are observed that do not modify long crack behaviour. Tests were conducted at 35 Hz on a servohydraulic machine. CT 75 (B=12 mm) specimens were used and crack length was measured on polished surface using a travelling microscope. Crack closure was measured by mean of a back-face gage using the differential compliance method. Two kind of tests were conducted : one with a constant R ratio of 0.1 and the other with a variable R ratio. Rvariable (Rvar) is a Kmax constant procedure where Kmin is slowly increased in order to avoid crack closure while reaching threshold.

Fatigue crack growth rate curves in air are presented in fig. 3 and fig. 4. On fig. 3 the effect of crack closure is readily seen by comparing the da/dN vs ΔK and the da/dN vs ΔK_{eff} curves. Fig. 4 shows a comparison between the effective curve at R0.1 and the Rvar curve in air. Crack growth rates have been presented elsewhere ; for futher details see Nadot and al. (1). Comparison plot on fig. 4 brings out the following points :

- for da/dN > 10^{-9} m/cycle the two curves are identical. It means that closure measurement at R0.1 reveals the same mechanical crack growth behaviour as does the closure-free propagation observed at Rvar.
- For da/dN < 10^{-9} m/cycle significant differences are noticed : threshold at Rvar is 3.5 MPa$\sqrt{m}$ while the effective threshold at R0.1 is 5 MPa$\sqrt{m}$. This difference is not due to a closure effect because curves plotted in fig. 4 are compared in term of effectives values. It seems to be related to the appearance of a thick oxide layer that cover 50% of the surface observed for the test performed at R0.1. The oxide formation which is favorised by the contact of the two cracked surfaces at R0.1 is not observed at Rvar. The

difference of threshold value is attributed to a local environment change at the crack tip. The active species contained in air (water vapour, hydrogen...) reaches the crack tip more easily for the test at Rvar than for the test at a constant R0.1 ratio where these elements are partially absorbed by the oxide layer protecting by this way the crack tip.

FATIGUE LIFE PREDICTION

Fatigue tests were conducted on as cast cylindrical samples in tension for load ratio R=0.1. Test was performed at room temperature at 35 Hz.

Fatigue crack propagation of natural short cracks

First the accuracy of applying FCG data determined on CT specimens to the propagation of a natural crack has been verified. A sample has been tested under constant amplitude loading with an alternating environment : air and high vacuum (2.10^{-4} Pa). This sequence air/vacuum has been repeated to failure with 10 000 cycles in air and 100 000 in vacuum. The successive change of environment acts as a crack front marker because of the difference between micromechanisms of crack propagation in air and vacuum, see ref. (1). Thus SEM observations give us the full crack front geometry and its evolution.

Fig. 5 gives an example of the crack front marked by the alternance air/vacuum. The number of cycle between the two marks has been calculated using the relation $\Delta K = 0.70\Delta\sigma\sqrt{\Pi a}$ from Levan and Royer (2) and integrating the Elber's da/dN vs ΔK_{eff} law determined at Rvar. The number of cycles applied in air between the two marks is 10 000. The result of the integration of the Elber's law gives a number of cycles of 12000 which is in very good agreement with experiment. For comparison, an estimation using the nominal da/dN vs ΔK Paris's relation leads to 190 000 cycles which is 19 times as high as the experimental value.

Growth rates of a natural short crack can be described using the Elber's law determined from the long FCG test at Rvar. It means that natural short cracks propagate without crack closure in agreement with results of other authors : T.Lindley and A.Pineau (3).

fatigue life calculation

Fatal cracks have been observed to initiate from dross defects close to the cast surface (example on fig. 2). To evaluate propagation stage the defect is considered as a pre-existent crack of depth a_i. The lowest value of ΔK initial for the five observed samples is 5.4 MPa$\sqrt{m}$ wich is superior to the threshold value for long crack at Rvar (3.5 MPa$\sqrt{m}$) so that propagation

law can be used. For each defect the relevant ΔK parameter from ref. (2) is used in relation with the geometry of the defect. Fatigue life is then calculated by integration of the Elber's law.

Fig. 6 shows the propagation period versus the experimental lifetime. It can be seen that these estimations are in good agreement with experiments for fatigue lives less than 200 000 cycles which corresponds to a stress level higher than 290 MPa. It means that for these stress levels crack initiation stage can be neglected and fatigue life can be described by propagation from casting defect as mentionned by Starkey and Irving (4). Results are in poor agreement with experimental data when stresses are lower than 290 MPa. Consequently, near the fatigue limit the whole fatigue life can not be described by a simple propagation period. For such stress levels, a significative part of lifetime is associated with an initiation stage of a crack around the defect which cannot be simply identified to a pre-existent microcrack.

Further tests and observations are needed to correlate stress level, crack depth and threshold value in order to understand the endurance limit concept in such materials.

CONCLUSION

- It is observed that the relation between the crack growth rate and the effective ΔK level can describe fatigue crack propagation of natural short crack on cylindrical samples.
- Assessments considering that the whole fatigue life can be described by the propagation of a crack strarting from an initial crack with a size and form equivalent to the initial defect are in good agreement with experimental values for high stress levels.
- At lower stress levels the present study brings out that a crack initiation stage have to be considered.

ACKNOWLEDGEMENTS

The financial and technical support of Renault SA for this study is greatfully acknowledged.

SYMBOLS USED

a = crack depth
B = thickness of the CT specimen
da/dN = crack growth rate
E = young modulus
K = stress intensity factor
ΔK_{eff} = effective stress intensity factor amplitude
$\Delta\sigma$ = stress amplitude
ΔK = stress intensity factor amplitude
σ_y = 0.2% yield strength
UTS = ultimate tensile strength
R = load ratio : R=Kmin/Kmax

REFERENCES

(1) Nadot, Y., Ranganathan, N.,Mendez, J. and Béranger, A.S. "fatigue crack propagation in spheroidal graphite cas iron (SGI)" to be published.

(2) Levan, A. and Royer, J. "part-circular surface cracks in round bars under tension, bending and twisting", Int. J. of Fract. vol. **61.**, pp. 71-99, 1993.

(3) T.Lindley and A.Pineau "Short crack effects in fracture and fatigue"Science et Génie des Mat. No 2 1995 pp.187-202

(4) M.S. Starkey and P.E. Irving "a comparison of the fatigue strength of machined and as cast surfaces of SGI" Int. J. Fat. July 1982 pp.129-136

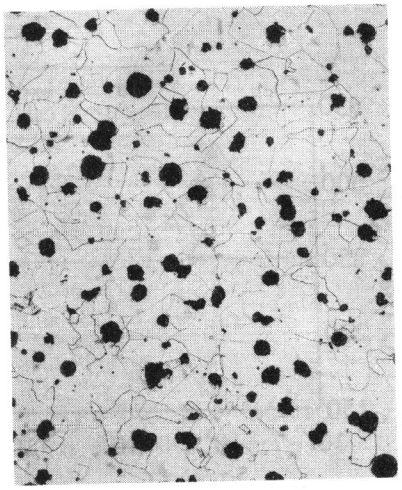

fig. 1 : microstructure of SGI

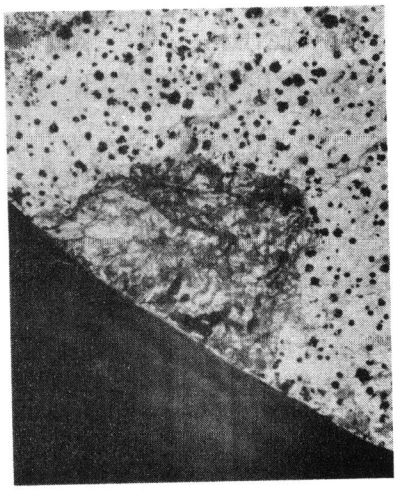

fig. 2 : surface dross defect

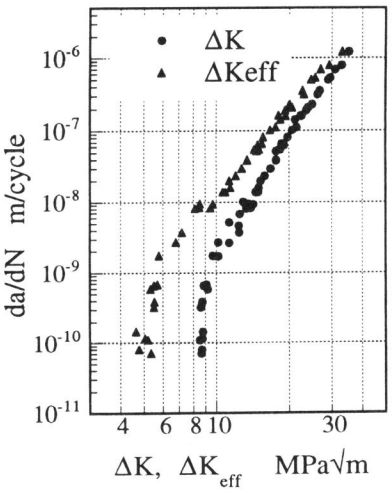

fig. 3 : fatigue crack propagation at R=0.1

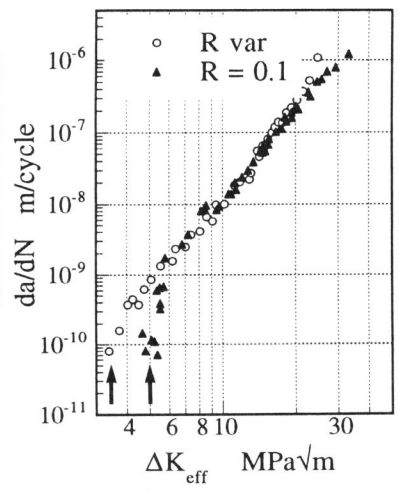

fig. 4 : comparison between effective threshold at Rvar and R=0.1

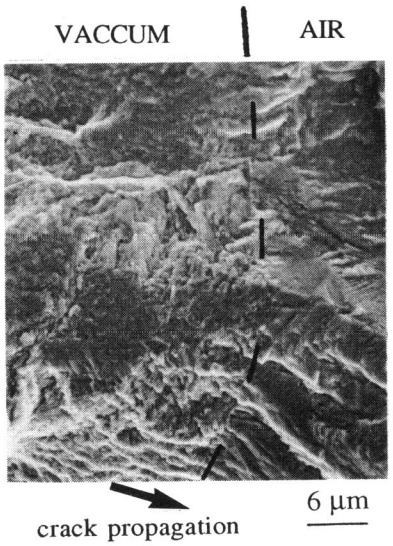

fig. 5 : crack front marked by the alternance air / vaccum

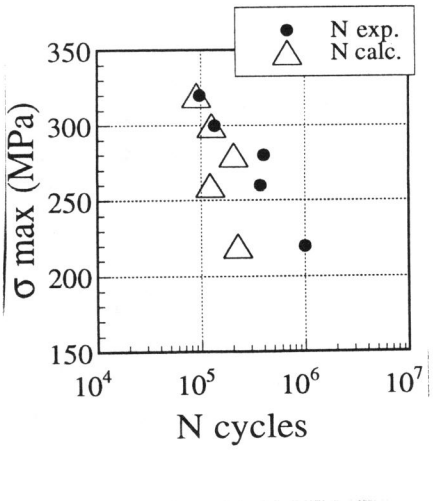

fig. 6 : comparison between calculated and experimental lifetime